CHIN. PHYS. LETT. Vol. 36, No. 5 (2019) 057402 **Express Letter**

# Superconductivity and Fermi Surface Anisotropy in Transition Metal Dichalcogenide $NbTe_2$ *

Xi Zhang(张玺)[1,2†], Tianchuang Luo(罗天创)[1,2†], Xiyao Hu(胡希瑶)[1], Jing Guo(郭静)[3], Gongchang Lin(林恭长)[3], Yuehui Li(李跃辉)[1,4], Yanzhao Liu(刘彦昭)[1,2], Xiaokang Li(李小康)[5,6], Jun Ge(葛军)[1,2], Ying Xing(邢颖)[7], Zengwei Zhu(朱增伟)[5,6], Peng Gao(高鹏)[1,2,4,8], Liling Sun(孙力玲)[3,9,10], Jian Wang(王健)[1,2,8,11**]

[1] *International Center for Quantum Materials, School of Physics, Peking University, Beijing 100871*
[2] *Collaborative Innovation Center of Quantum Matter, Beijing 100871*
[3] *Institute of Physics and Beijing National Laboratory for Condensed Matter Physics, Chinese Academy of Sciences, Beijing 100190*
[4] *Electron Microscopy Laboratory, School of Physics, Peking University, Beijing 100871*
[5] *School of Physics, Huazhong University of Science and Technology, Wuhan 430074*
[6] *Wuhan National High Magnetic Field Center, Huazhong University of Science and Technology, Wuhan 430074*
[7] *Department of Materials Science and Engineering, School of New Energy and Materials, China University of Petroleum, Beijing 102249*
[8] *Beijing Academy of Quantum Information Sciences, Beijing 100193*
[9] *University of Chinese Academy of Sciences, Beijing 100190*
[10] *Songshan Lake Materials Laboratory, Dongguan 523808*
[11] *CAS Center for Excellence in Topological Quantum Computation, University of Chinese Academy of Sciences, Beijing 100190*

(Received 3 April 2019)

*Transition metal dichalcogenides, featuring layered structures, have aroused enormous interest as a platform for novel physical phenomena and a wide range of potential applications. Among them, special interest has been placed upon $WTe_2$ and $MoTe_2$, which exhibit non-trivial topology both in single layer and bulk as well as pressure induced or enhanced superconductivity. We study another distorted 1T material $NbTe_2$ through systematic electrical transport measurements. Intrinsic superconductivity with onset transition temperature ($T_c^{\rm onset}$) up to 0.72 K is detected where the upper critical field ($H_c$) shows unconventional quasi-linear behavior, indicating spin-orbit coupling induced p-wave paring. Furthermore, a general model is proposed to fit the angle-dependent magnetoresistance, which reveals the Fermi surface anisotropy of $NbTe_2$. Finally, non-saturating linear magnetoresistance up to 50 T is observed and attributed to the quantum limit transport.*

*PACS:* 74.20.Rp, 74.70.Ad, 74.25.F−, 71.18.+y DOI: 10.1088/0256-307X/36/5/057402

Transition metal dichalcogenides (TMDs) are a group of materials with chemical composition $MX_2$ (M is a transition metal and X=S, Se, Te), which have aroused great research interest recently. An important feature of TMDs is that many of them are of layered structures,[1] where layers are stacked together by relatively weak van der Waals interaction, enabling applications ranging from nanoelectronics to nanophotonics.[2] More importantly, a variety of novel physical phenomena such as charge density wave (CDW),[3] Ising superconductivity,[4,5] non-trivial band topology[6–8] and potential topological superconductivity[9] have also been observed in TMDs.

Among layered TMDs, distorted 1T type materials are of particular significance. In a single layer, the 1T structure is typically unstable and will undergo spontaneous structural distortion to form period doubling of metal chains.[7] The resultant single-layer structure may be 1T′ or 1T″. In the 1T′ structure, such period doubling is expected to lower the metal $d$ orbital below chalcogenide $p$ orbital, leading to band inversion and quantum spin hall insulator (QSHI) state.[7] The distorted layers can stack in either orthorhombic (Td phase) or monoclinic fashion (1T′ and 1T″ phase).[10] As in Td-$MoTe_2$ and $WTe_2$, orthorhombic AB stacking results in non-trivial topology in the bulk materials, as identified by the type-Ⅱ Weyl semimetal phase.[6] On the other hand, monoclinic stacking of 1T″ layers, which may also host novel physical properties, has been rarely studied in theory and experiment.

$NbTe_2$ is a typical material of monoclinic 1T″ structure,[1,11] where quasi-1D triple metal chains are formed, different from the double chains in $WTe_2$. Experimental studies on $NbTe_2$ electronic structure have revealed that its lattice distortion arises from the Fermi surface (FS) nesting and electron-phonon coupling.[12] More recently, $NbTe_2$ was proposed as a candidate of semimetal with topological protected

*Supported by the National Basic Research Program of China under Grant Nos 2018YFA0305600 and 2017YFA0303302, the National Natural Science Foundation of China under Grant Nos 11888101, 11774008, 11704414 and 11427805, the Strategic Priority Research Program of Chinese Academy of Sciences under Grant No XDB28000000, and Beijing Natural Science Foundation (Z180010).

†These authors contributed equally to this work.

**Corresponding author. Email: jianwangphysics@pku.edu.cn

© 2019 Chinese Physical Society and IOP Publishing Ltd

band crossing[13] and signatures of linear dispersion band have been observed.[14] In such a topological semimetal, the search for superconductivity (SC) is of great significance. Magnetic susceptibility measurement has shown that $NbTe_2$ is an intrinsic superconductor with lower critical field ($H_{c1}$) less than 0.5 Oe at 0.40 K.[15] However, transport measurement on SC in $NbTe_2$ has been rarely reported, so that characteristics of the SC and its relation to topology are unavailable.

In this Letter, we report a systematic electrical transport study on SC and electronic structures of the 1T″ monoclinic TMD material $NbTe_2$. High quality single crystals of $NbTe_2$ are prepared by chemical vapor transport technique, whose chemical composition and crystal quality are checked by energy dispersive x-ray spectroscopy (EDS), x-ray diffraction (XRD) and high-angle annular dark-field (HAADF) scanning transmission electron microscopy (STEM). Intrinsic SC is clearly observed with $T_c^{onset}$ around 0.72 K, higher than that in Td-$MoTe_2$.[10] The temperature dependence of $H_c$ shows unconventional quasi-linear behavior, indicating contribution from spin-orbit coupling (SOC) induced p-wave paring. The FS of $NbTe_2$ is analyzed by magnetotransport measurement. We propose a new model to explain the observed angle-dependent magnetoresistance, which improves the fitting to the experimental data compared with the traditional formula. Moreover, a linear magnetoresistance persisting up to 50 T is detected, which is consistent with the previous results up to 9 T[14] and may originate from quantum limit transport.

In our experiment, high-quality $NbTe_2$ single crystal was grown by chemical vapor transport technique.[16] Nb and Te powders were mixed at a stoichiometric ratio and sealed in an evacuated tube after pressurization. The mixture was then heated to 520℃ and kept for 92 hours. After slowly cooling down to room temperature, the obtained substance was rigorously shaken and sealed with iodine in another tube. The tube was then placed coaxially in a multi-zone furnace. The growth temperature and reaction temperature were respectively set to 850℃ and 920℃ and crystal was grown for 9 days. On slowly cooling to room temperature, large and shiny crystals were obtained (inset of Fig. 1(c)). The atomic ratio of prepared crystal was checked by EDS to be exact 1:2. The layered structure of $NbTe_2$ was studied by HAADF-STEM, where parallel atomic layers and lattice distortion within layer are clearly visible (Fig. 1(a)). Single crystal character of our sample is further checked by XRD of (00$l$) crystalline plane (Fig. 1(b)). These results confirm that we have prepared high-quality 1T″ $NbTe_2$ single crystal.

Electrical transport measurement was performed in a physical property measurement system (PPMS-16 T) made by Quantum Design company with standard four/six-probe configuration. The current is applied in $ab$ plane and magnetic field is always perpendicular to the current. Resistivity $\rho$ of $NbTe_2$ as a function of temperature $T$ from 400 K to 2 K is shown in Fig. 1(c). The resistivity decreases with the decrease of temperature and saturates to around 0.05 mΩ·cm below 5 K, which is a typical metallic behavior and is similar to other TMD materials such as $WTe_2$[17,18] and $IrTe_2$.[19] The residual resistivity ratio defined as RRR $= \frac{\rho(300\,\mathrm{K})}{\rho(2\,\mathrm{K})}$ is around 7.8. In our measured temperature range, the 1T″-Td structural phase transition as observed in $MoTe_2$[10] is not detected. As a result, $NbTe_2$ serves as a unique platform to study distorted 1T structure properties in lower symmetry monoclinic phases.

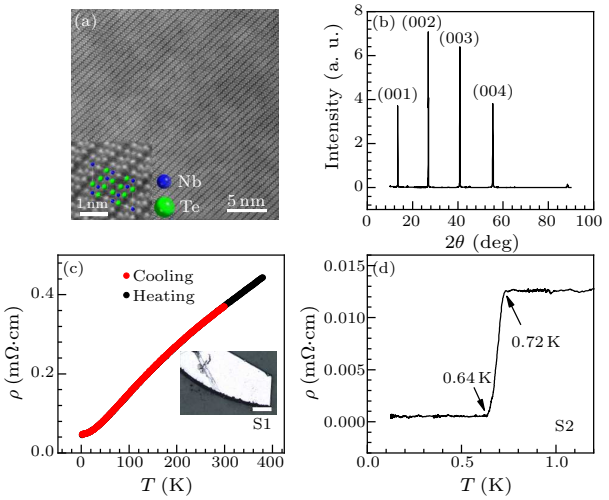



**Fig. 1.** Characterization and $\rho$–$T$ behavior of $NbTe_2$. (a) The HAADF-STEM image of $NbTe_2$ viewed from [010] direction, where the scale bar represents 5 nm. Inset is the enlarged view of the HAADF image overlaid with the atomistic model. Blue balls: Nb; green balls: Te; scale bar: 1 nm. (b) XRD of (00$l$) surface of single crystal $NbTe_2$. Labels assign peaks to the corresponding crystalline surfaces. (c) Resistivity as a function of temperature of $NbTe_2$ down to 2 K. Red and black curves indicate the data obtained during cooling and heating process. No signal of structural phase transition is observed. Inset is an optical picture of the $NbTe_2$ sample, where the scale bar represents 0.5 mm. (d) SC transition in $\rho$–$T$ behavior. Labels indicate zero and onset transition temperature.

SC in $WTe_2$ appears only under high pressure.[17,18] We observed intrinsic SC in $NbTe_2$ with $T_c^{onset}$ varying around 0.3 K to 0.72 K among different samples. SC transition at zero field is shown in Fig. 1(d). Resistivity starts to drop sharply at onset critical temperature 0.72 K and reaches zero resistivity within experimental resolution at 0.64 K. The resistivity drop can be suppressed by magnetic field, as shown in Figs. 2(a), 2(b), 2(d) and 2(e), which further signals SC transition. Magnetotransport measurements were carried out with magnetic field applied perpendicular and parallel to the $NbTe_2$ layer. We define upper critical field $H_c$ as the magnetic field when resistivity reaches half of its normal value, and its relation to temperature is shown in Fig. 2(c) and 2(f). For perpendicular magnetic field, the measured $H_c$–$T$ behavior is well captured by the model for spin-triple p-wave superconductors[20,21]

and deviates from the weak-coupling Werthamer–Helfand–Hohenberg (WHH) formula at the dirty limit[22] (Fig. 2(c)). Zero-temperature critical field estimated by the polar p-wave model is 295 Oe. For the parallel magnetic field, $H_c$–$T$ exhibits a more linear behavior and shows higher zero temperature critical field than that expected from the polar p-wave model (Fig. 2(f)). In this case, the orbital limiting field $H_{orb} = 0.69(-dH_c/dT)_{T_c}$ is around 600 Oe, which is clearly smaller than the experimental zero-temperature critical field $H_{c\|}$ and consequently indicates that the SOC cannot be neglected.[23] SC in $NbTe_2$ shows clear anisotropy, since measured $H_{c\|}$ is over twice that of the out-of-plane value $H_{c\perp}$, which is expected for a layered superconductor.[24,25] According to the proposed scaling approach to anisotropic superconductors, effective magnetic field is introduced by $\tilde{H} = H(\cos^2\theta + \gamma^{-2}\sin^2\theta)^{\frac{1}{2}}$, where $\theta = 0°$ corresponds to out-of-plane direction and $\gamma$ is the mass anisotropy.[25,26] By this analysis, $\gamma$ is estimated by the ratio between parallel and perpendicular zero temperature critical field $H_{c\|}/H_{c\perp}$ to be around 2.48.

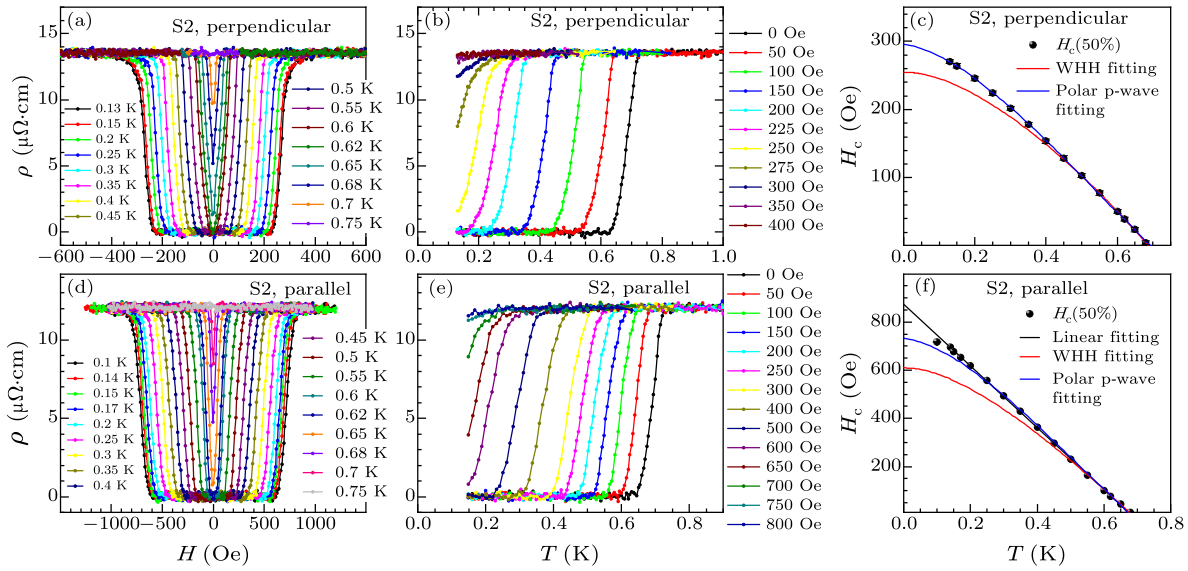



**Fig. 2.** Magnetotransport properties in superconducting $NbTe_2$. (a) Resistivity as a function of perpendicular magnetic field at various temperatures. (b) The $\rho$–$T$ curves under various perpendicular magnetic fields. (c) Critical perpendicular magnetic field as a function of temperature for $NbTe_2$. Red and blue curves are the WHH and polar p-wave fits to the data, respectively. (d)–(f) Results for parallel magnetic field. Black curve in (f) is linear fitting.

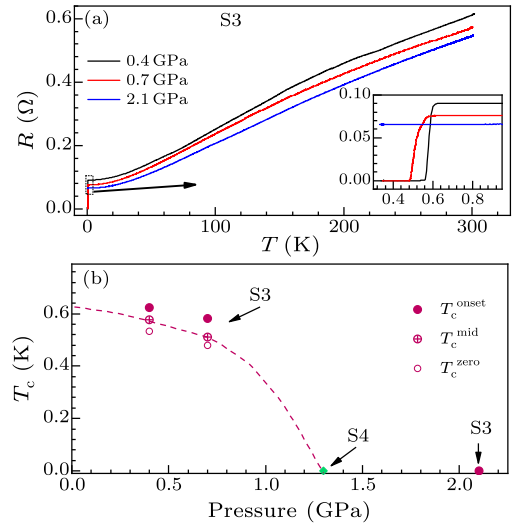



**Fig. 3.** SC in $NbTe_2$ under hydrostatic pressure. (a) The $R$–$T$ behavior of $NbTe_2$ under various hydrostatic pressures. Inset is the zoom-in SC transition. (b) The relation between $T_c$ and hydrostatic pressure. $T_c = 0$ indicates no SC observed.

It is also of interest whether the superconducting temperature of the superconducting $NbTe_2$ can be enhanced by pressure, as observed from $WTe_2$[17,18] and $MoTe_2$.[10] We performed transport measurements of $NbTe_2$ single crystals under hydrostatic pressure up to 2.1 GPa for the two samples (S3 and S4 in Fig. 3). The resistance $R$ of S3 as a function of $T$ under various pressures is shown in Fig. 3(a). The sample resistivity decreases with the increase of hydrostatic pressure. However, the SC transition temperature $T_c$ is simultaneously suppressed (inset in Fig. 3(a)). At 2.1 GPa, no sign of SC transition is observed in S3. The relation between $T_c$ and hydrostatic pressure is summarized in Fig. 3(b). Over the same pressure range, $T_c$ increases dramatically in Td-$MoTe_2$, which is discovered to be related to the suppression of 1T′-Td structural phase transition.[10] Nevertheless, this transition is absent in $NbTe_2$. In $WTe_2$, SC only occurs at much higher pressure (around 10 GPa)[17] when the Fermi surface of $WTe_2$ is remarkably reconstructed. As a result, although hydrostatic pressure seems to be unfavorable for observed SC in $NbTe_2$, higher pressure is still highly desired to see if another superconducting state can be induced.

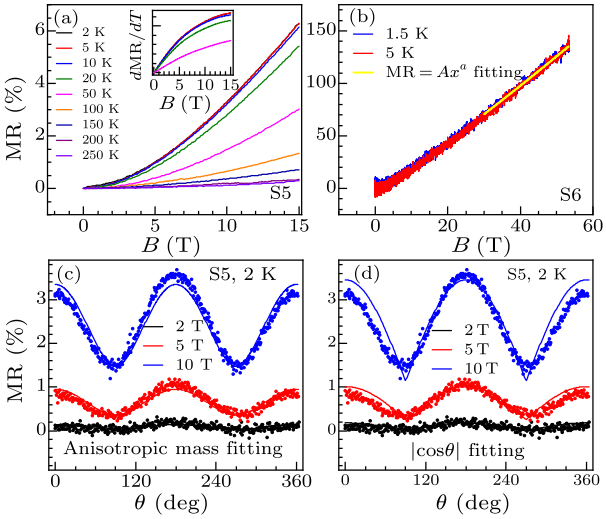



**Fig. 4.** Magnetoresistance of $NbTe_2$. (a) MR as a function of perpendicular magnetic field at various temperatures. Inset is the first order derivative $d\mathrm{MR}/dT$, which shows a transition from linear to saturation with increasing magnetic field, indicating a quadratic to linear transition of MR–$B$ behavior. (b) MR as a function of perpendicular magnetic field up to 50 T measured in a pulsed magnet. The yellow line is the power law fitting to the data at 1.5 K. (c) MR as a function of magnetic field direction $\theta$ at 2 K and $B = 2$, 5, 10 T. Here $\theta = 0°$ is the out-of-plane direction and $\theta = 90°$ the in-plane direction. Solid curves are fitting to the data with the anisotropic mass model. (d) Fitting to the data in (c) with the traditional $|\cos\theta|$ model.

Magnetotransport measurements above $T_c$ provide intriguing insight into the electronic structure of $NbTe_2$. Figure 4(a) shows the longitudinal magnetoresistance ($\mathrm{MR} = \frac{\rho(B)-\rho(B=0)}{\rho(B=0)} \times 100\%$) measured at various temperatures. The MR exhibits a non-saturating behavior and is suppressed by temperature. The first order derivative of MR as a function of $B$ (inset of Fig. 4(a)) is linear at low field and tends to saturation with the increase of magnetic field, which indicates a transition from quadratic to linear dependence.[14,27] To uncover the origin of the novel linear magnetoresistance behavior, the information of $NbTe_2$ Fermi surface is necessary. Thus, we carried out angle-dependent magnetoresistance measurements. When the magnetic field is rotated from out-of-plane ($\theta = 0°$) to in-plane direction ($\theta = 90°$), the MR shows a monotonic decreasing behavior. Figures 4(c) and 4(d) show the angle-dependent MR at different magnetic fields. This behavior is reminiscent of what has been observed in other quasi-2D compounds[28,29] and topological insulators,[30] which was typically fitted with a $|\cos\theta|$ model. The model was motivated by the consideration that for 2D or quasi-2D FS, the transport behavior will mainly respond to the magnitude of out-of-plane component of the magnetic field ($B|\cos\theta|$). However, the argument fails to take into account of the fact that the variation amplitude of MR with $\theta$ also depends on $B$. The fitting formula used in aforementioned references is actually $f(B)|\cos\theta|$, where the explicit form and physical picture of amplitude function $f(B)$ are unclear. Moreover, $|\cos\theta|$ fitting forms a sharp dip at $\theta = 90°$ and 270° and thus cannot fit the experimental data well. In order to overcome the limitation of the $|\cos\theta|$ model, we propose a more general fitting formula based on the anisotropy of 3D FS.[31]

As has been proposed for 3D anisotropic FS, longitudinal magnetoresistance follows the scaling behavior similar to that of anisotropic superconductor, $\mathrm{MR}(\theta, B) = \mathrm{MR}(\varepsilon_\theta B)$, where $\varepsilon_\theta = (\cos^2\theta + \gamma^{-2}\sin^2\theta)^{1/2}$.[31] Considering the power rule of MR revealed in Fig. 4(a), we suppose a phenomenological model $\mathrm{MR}(\theta, B) = A(\varepsilon_\theta B)^\alpha + C$ ($A$ and $C$ are constants), which combines the angular and field dependence. The model turns out to fit our experimental data better than the traditional $|\cos\theta|$ formula (solid lines in Fig. 4(c) and Fig. 4(d)). The fitting gives $\alpha = 1.96$, 1.74 and 1.69 for $B = 2$, 5 and 10 T, respectively. Indeed, the MR follows a quadratic law around $B = 2$ T and the power decreases gradually with the increase of magnetic field (inset of Fig. 4(a)). The mass anisotropy $\gamma$ obtained by fitting lies between 1.73 and 3.51, which exhibits a large fitting error whereas is consistent with the $\gamma$ value (2.48) obtained by analysis of anisotropic SC. The value is also comparable to that of $WTe_2$.[31] The fitting at 10 T does not perfectly reproduce experimental data, which may originate from the variation of power $\alpha$ over the range of effective magnetic field $\varepsilon_\theta B$. Our analysis shows that the transport behavior of $NbTe_2$ is dominated by an anisotropic 3D FS for magnetic field below 10 T. We remark that the traditional $|\cos\theta|$ model corresponds to the $\alpha = 1$ and $\gamma \to \infty$ case in our model. In this case, the sample should lie in linear magnetoresistance region and have a very high anisotropy, which is not suitable for our experimental condition.

Hall resistivity as a function of magnetic field at various temperatures is shown in Fig. 5(a). The linear behavior up to 15 T after antisymmetrization indicates a single hole pocket. Carrier density is calculated from linear fitting by $n = 1/R_\mathrm{H}e$ ($e$ is the elementary charge and $R_\mathrm{H}$ the Hall coefficient) as shown in Fig. 5(b). At 2 K, $n \approx 8 \times 10^{20}\,\mathrm{cm}^{-3}$, corresponding to a rather large FS and is responsible for the metallic behavior of $NbTe_2$. The low temperature mobility of S2 is around $120\,\mathrm{cm}^2/(\mathrm{V{\cdot}s})$. The broadening of Landau levels thus smears out quantum oscillation since $\omega_c\tau = \mu B < 1$.[32]

We then turn to analyze the origin of non-saturating magnetoresistance in $NbTe_2$. Considering the large FS revealed by our analysis, it is natural to suspect the non-saturating magnetoresistance originate from an open FS. However, careful theoretical consideration suggests that MR from open FS will exhibit $H^{2/3}$ dependence for uncompensated metals (with unequal density of electrons and holes).[33,34] In order to examine this possibility, we perform magnetoresistance measurement up to 50 T in pulsed magnetic field at Wuhan National High Magnetic Field Center. As shown in Fig. 4(b), the magnetoresis-

tance remains unsaturated over the whole measured range. By fitting to a power formula (yellow curve in Fig. 4(b)) MR $= AB^{\alpha}$, we obtain $\alpha \approx 1.1$ for the MR at 1.5 K with the magnetic field larger than 30 T. The result obviously deviates from the open FS model. Two alternative explanations may be quantum limit transport or disorder effect. Quantum limit transport requires $n \ll (\frac{eB}{\hbar})^{3/2}$,[33] which is not fulfilled for the large pocket discussed above. If another small pocket can reach the quantum limit and dominate over the large pocket in conductance, quantum linear magnetoresistance can also occur.[33] On the other hand, the disorder induced linear magnetoresistance, as the case in doped $Ag_2Se$ and $Ag_2Te$,[35,36] is unlikely to be the explanation because the linear magnetoresistance in $NbTe_2$ is strongly suppressed with the increase of temperature, which is different from the typical behavior of disorder induced linear magnetoresistance.[35,37] Also, the high quality of our sample does not seem to permit strong disorder or inhomogeneity. As a result, quantum limit transport is the possible explanation for the observed linear and non-saturating magnetoresistance up to 50 T in $NbTe_2$.

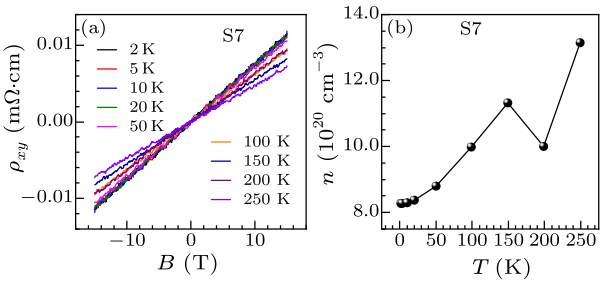



**Fig. 5.** Hall signal and carrier density of $NbTe_2$. (a) Hall resistivity as a function of magnetic field at various temperatures. (b) Carrier density as a function of temperature obtained by linear fitting of (a).

Finally, we discuss the relation between SC and FS structures in $NbTe_2$. Since a large 3D anisotropic FS is revealed by transport measurement, whose mass anisotropy $\gamma$ is similar to that of SC, SC at the temperature lower than 0.72 K is likely to originate from Cooper pairing in the same pocket. The measured single band quasi-linear $H_c$–$T$ behavior indicates that strong SOC gives rise to a p-wave pairing contribution to the SC state in $NbTe_2$. However, besides a large hole pocket, ultrahigh magnetic field measurements suggest that a small pocket may also exist. In analogy to $MoTe_2$[9,10] and $WTe_2$,[17,18] with appropriate FS engineering, a multi-band SC phase may emerge in $NbTe_2$ with potential non-trivial topology.

In conclusion, by performing transport measurements on high-quality $NbTe_2$ crystals, we have observed intrinsic SC with $T_c^{onset}$ up to 0.72 K. The temperature dependence of $H_c$ implies the contribution from the p-wave paring induced by SOC. The electronic structure of $NbTe_2$ is revealed by magnetotransport measurement. Based on anisotropic FS and power law of MR, we propose a phenomenological model to fit our angle-dependent magnetoresistance results. Ultrahigh magnetic field measurements show linear magnetoresistance up to 50 T. Its quantum limit origin suggests the existence of a small Fermi pocket. In comparison to $MoTe_2$ and $WTe_2$, our work indicates that a potential multi-band superconducting state in $NbTe_2$ could be achieved by modulating FS such as applying higher pressure or doping the sample. This work calls on further calculation and experimental investigations on the novel electronic properties of 1T″ TMD materials.

We gratefully acknowledge Gatan for the technique assistance. The authors acknowledge Electron Microscopy Laboratory in Peking University for use of the Cs corrected electron microscope.

## References

[1] Wilson J A and Yoffe A D 1969 *Adv. Phys.* **18** 193
[2] Manzeli S, Ovchinnikov D, Pasquier D, Yazyev O V and Kis A 2017 *Nat. Rev. Mater.* **2** 17033
[3] Wilson J A, Di Salvo F J and Mahajan S 1975 *Adv. Phys.* **24** 117
[4] Lu J M, Zheliuk O, Leermakers I, Yuan N F Q, Zeitler U, Law K T and Ye J T 2015 *Science* **350** 1353
[5] Xing Y, Zhao K, Shan P, Zheng F, Zhang Y, Fu H, Liu Y, Tian M, Xi C, Liu H, Feng J, Liu X, Ji S, Chen X, Xue Q K and Wang J 2017 *Nano Lett.* **17** 6802
[6] Soluyanov A A, Gresch D, Wang Z, Wu Q, Troyer M, Dai X and Bernevig B A 2015 *Nature* **527** 495
[7] Qian X, Liu J, Fu L and Li J 2014 *Science* **346** 1344
[8] Wu S, Fatemi V, Gibson Q D, Watanabe K, Taniguchi T, Cava R J and Jarillo-Herrero P 2018 *Science* **359** 76
[9] Li Y, Gu Q, Chen C, Zhang J, Liu Q, Hu X, Liu J, Liu Y, Ling L, Tian M, Wang Y, Samarth N, Li S, Zhang T, Feng J and Wang J 2018 *Proc. Natl. Acad. Sci. USA* **115** 9503
[10] Qi Y P, Naumov P G, Ali M N, Rajamathi C R, Schnelle W, Barkalov O, Hanfl, M, Wu S C, Shekhar C, Sun Y, Suss V, Schmidt M, Schwarz U, Pipel E, Werner P, Hillebr, R, Forster T, Kampert E, Parkin S, Cava R J, Felser C, Yan B H and Medvedev S A 2016 *Nat. Commun.* **7** 11038
[11] Brown B E 1966 *Acta Crystallogr.* **20** 264
[12] Battaglia C, Cercellier H, Clerc F, Despont L, Garnier M G, Koitzsch C, Aebi P, Berger H, Forro L and Ambrosch-Draxl C 2005 *Phys. Rev. B* **72** 195114
[13] Tang F, Po H C, Vishwanath A and Wan X 2019 *Nature* **566** 486
[14] Chen H X, Li Z L, Fan X, Guo L W and Chen X L 2018 *Solid State Commun.* **275** 16
[15] Nagata S, Abe T, Ebisu S, Ishihara Y and Tsutsumi K 1993 *J. Phys. Chem. Solids* **54** 895
[16] Vaidya R, Bhatt N, Patel S G, Jani A R, Garg A, Vijayakumar V and Godwal B K 2003 *High Press. Res.* **23** 379
[17] Kang D F, Zhou Y Z, Yi W, Yang C L, Guo J, Shi Y G, Zhang S, Wang Z, Zhang C, Jiang S, Li A G, Yang K, Wu Q, Zhang G M, Sun L L and Zhao Z X 2015 *Nat. Commun.* **6** 7804
[18] Pan X C, Chen X L, Liu H M, Feng Y Q, Wei Z X, Zhou Y H, Chi Z H, Pi L, Yen F, Song F Q, Wan X G, Yang Z R, Wang B G, Wang G H and Zhang Y H 2015 *Nat. Commun.* **6** 7805
[19] Zhang X, Wang J, Liu Y, Zheng W and Wang J 2017 *J. Phys. Chem. Solids* (accepted)
[20] Scharnberg K and Klemm R A 1980 *Phys. Rev. B* **22** 5233
[21] Xing Y, Wang H, Li C K, Zhang X, Liu J, Zhang Y W, Luo J W, Wang Z Q, Ling L S, Tian M L, Jia S, Feng J, Liu X J, Wei J and Wang J 2016 *npj Quantum Mater.* **1** 16005
[22] Werthamer N R, Helf E and Hohenberg P C 1966 *Phys. Rev.* **147** 295
[23] Xiao H, Hu T, Liu T W, Zhu Y L, Li P G, Mu G, Su J, Li

K and Mao Z Q 2018 *Phys. Rev. B* **97** 224511
[24] Xing Y, Shao Z B, Ge J, Wang J H, Zhu Z W, Liu J, Wang Y, Zhao Z Y, Yan J Q, Mandrus D, Yan B H, Liu X J, Pan M H and Wang J 2018 arXiv:1805.10883v3[cond-mat.supr-con]
[25] Morris R C, Coleman R V and Rajendra R 1972 *Phys. Rev. B* **5** 895
[26] Blatter G, Geshkenbein V B and Larkin A I 1992 *Phys. Rev. Lett.* **68** 875
[27] Wang Q Y, Zhang W H, Chen W W, Xing Y, Sun Y, Wang Z Q, Mei J W, Wang Z F, Wang L L, Ma X C, Liu F, Xue Q K and Wang J 2017 *2D Mater.* **4** 034004
[28] Wang K F, Graf D, Lei H C, Tozer S W and Petrovic C 2011 *Phys. Rev. B* **84** 220401
[29] Zhan Y, Liu H, Yan J, An W, Liu J, Zhang X, Wang H, Liu Y, Jiang H, Li Q, Wang Y, Li X, Mandrus D, Xie X, Pan M and Wang J 2015 *Phys. Rev. B* **92** 041104
[30] Tang H, Liang D, Qiu R L J and Gao X P A 2011 *ACS Nano* **5** 7510
[31] Thoutam L R, Wang Y L, Xiao Z L, Das S, Luican-Mayer A, Divan R, Crabtree G W and Kwok W K 2015 *Phys. Rev. Lett.* **115** 046602
[32] Shoenberg D 1984 *Magnetic Oscillations in Metals* (New York: Cambridge University Press) p 61
[33] Abrikosov A A 2000 *Europhys. Lett.* **49** 789
[34] Zhang T, Jiang Y, Song Z, Huang H, He Y, Fang Z, Weng H and Fang C 2019 *Nature* **566** 475
[35] Xu R, Husmann A, Rosenbaum T F, Saboungi M L, Enderby J E and Littlewood P B 1997 *Nature* **390** 57
[36] Parish M M and Littlewood P B 2003 *Nature* **426** 162
[37] Hu J S and Rosenbaum T F 2008 *Nat. Mater.* **7** 697